

AD-A089 207

WASHINGTON UNIV SEATTLE DEPT OF MINING METALLURGICAL--ETC F/6 11/5
STRESS-INDUCED EFFECTS UPON THE STRUCTURE AND PROPERTIES OF CAR--ETC(U)
JUL 80 D B FISCHBACH, K KOMAKI DAAG29-76-G-0169

UNCLASSIFIED

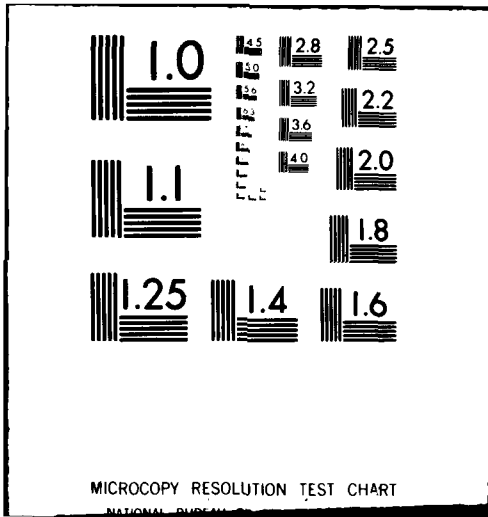
ARO-13485.6-MS

NL

1
2
3
4
5
6
7
8
9
10



END
DATE
FILMED
10-80
DTIC



MICROCOPY RESOLUTION TEST CHART

NATIONAL BUREAU OF STANDARDS

AD A089207

(2) ARO 13485.6-MS
LEVEL III

STRESS-INDUCED EFFECTS UPON THE STRUCTURE AND PROPERTIES
OF CARBON FIBERS

FINAL TECHNICAL REPORT

D. B. Fischbach, K. Komaki, S. Srinivasagopalan

31 July 1980

DTIC
ELECTE
SEP 15 1980
S D C

U. S. Army Research Office
Grant # DAAG29 76 G 0169; ¹⁴ 78 G 0142
(1 March 1976 - 31 May 1980)

Department of Mining, Metallurgical & Ceramic Engineering
UNIVERSITY OF WASHINGTON FB-10
Seattle, WA 98195

APPROVED FOR PUBLIC RELEASE
DISTRIBUTION UNLIMITED

UDC FILE COPY

80 9 15 007

SUMMARY

Microstructures and structural development with heat treatment temperature HTT (≤ 1000 to ~ 3000 C) of carbon fibers from pitch (P), rayon (R), polyacrylonitrile (PAN) and pitch mesophase (PM) were characterized by diamagnetic susceptibility and scanning electron microscopy, and the dynamic torsional behavior (~ 1 Hz) and electrical resistance characteristics of individual fibers were surveyed. Much of the qualitative behavior is common to fibers from all precursor types and to stratic (hexagonal layer) carbon materials generally, but the quantitative property levels are, of course, structure-sensitive.

The torsional (longitudinal shear) modulus is much lower than and insensitive to longitudinal Young's modulus. It depends on fiber transverse layer orientation texture and precursor type in general agreement with anisotropic elasticity considerations, ranging from ~ 9 GPa for PM fiber with a radial texture component to ~ 35 GPa for PAN fiber with a strongly circumferential texture. Damping (log decrement) decreases with $\text{HTT} < 2000$ C to $\approx 10^{-3}$, and is amplitude independent and insensitive to measurement temperature in the range -50 to $+50$ C. The torsional modulus decreases and damping increases reversibly and approximately linearly with the square of static torsional bias strain. This effect increases in magnitude with longitudinal layer orientation and is attributed to elastic decoupling between fiber substructural elements.

The electrical resistivity ρ of fibers is typically about one milli-ohm-cm, but ranges with precursor type and HTT about an order of magnitude above (low modulus R,P) and below (graphitized PM) this value. Layer structure development/graphitization and longitudinal orientation contribute about equally in determining ρ . Residual nitrogen defects in PAN, which strongly influence magnetic behavior, have no obvious effect on resistivity; but fiber ρ rises steeply with decreasing $\text{HTT} < 1200$ C, as for all carbon materials. The measurement temperature dependence was characterized by the temperature coefficient of resistance (0 to $+50$ C) and by the ratio of the resistance at liquid nitrogen temperature to that at 0 C: It is negative for all fiber types; and the magnitude decreases to a minimum then increases toward a maximum with increasing HTT and structural perfection. This behavior, which is not well understood, appears to be common to all stratic carbons (with sufficient structural development, as in graphitized pyrocarbons, the sign reverses to positive). The tensile piezoresistance behavior is reversible at low strains and typically positive and approximately linear for most fibers, but it decreases with increasing structural perfection and abruptly becomes negative at low strain levels in high modulus fibers (especially PM). In general, the piezoresistance may be modeled phenomenologically as the sum of positive and negative components. Analysis of possible contributing mechanisms suggests that positive geometrical effects (elongation plus transverse Poisson's contraction) may combine with the negative influence of stress-induced layer orientation in low to medium modulus fibers. However, these mechanisms must diminish in importance with increasing structural anisotropy and preferential conduction along the layers. The net negative effects in highly oriented fibers may result from carrier mobility increase (e.g., reduced scattering resulting from layer unwrinkling). Opening of internal contacts can cause the positive upturn that often precedes failure, and may contribute at lower strains as well.

THE VIEWS, OPINIONS, AND/OR FINDINGS CONTAINED IN THIS REPORT ARE THOSE OF THE AUTHORS AND SHOULD NOT BE CONSTRUED AS AN OFFICIAL DEPARTMENT OF THE ARMY POSITION, OR DECISION, UNLESS SO DESIGNATED BY OTHER DOCUMENTATION.

UNCLASSIFIED

19 AEP 1

SECURITY CLASSIFICATION OF THIS PAGE (When Data Entered)

REPORT DOCUMENTATION PAGE		READ INSTRUCTIONS BEFORE COMPLETING FORM
1. REPORT NUMBER (19) 134 85.6-MS /	2. GOVT ACCESSION NO. AD-A089 207	3. RECIPIENT'S CATALOG NUMBER
4. TITLE (and Subtitle) (6) STRESS-INDUCED EFFECTS UPON THE STRUCTURE AND PROPERTIES OF CARBON FIBERS.		5. TYPE OF REPORT & PERIOD COVERED Final Technical Report (1 Mar '76 - 31 May 1980)
7. AUTHOR(s) (10) D.B. Fischbach, K. Komaki, S. Srinivasagopalan David Kunio Seshadri		6. PERFORMING ORG. REPORT NUMBER
PERFORMING ORGANIZATION NAME AND ADDRESS Dept. of Mining, Metallurgical & Ceramic Engineering UNIVERSITY OF WASHINGTON FB-10 Seattle, WA 98195		8. CONTRACT OR GRANT NUMBER(s) DAAG29 76 G 0169 " 78 G 0142
11. CONTROLLING OFFICE NAME AND ADDRESS U. S. Army Research Office Post Office Box 12211 Research Triangle Park, NC 27709		10. PROGRAM ELEMENT, PROJECT, TASK AREA & WORK UNIT NUMBERS (13) DAAG-29-76-G-0169 DAAG-29-78-G-0142
14. MONITORING AGENCY NAME & ADDRESS (if different from Controlling Office) (9) Final technical rept. 1 Mar 76-31 May 80.		12. REPORT DATE 31 Jul 80
		13. NUMBER OF PAGES 13
		15. SECURITY CLASS. (of this report) Unclassified (12) 166
		15a. DECLASSIFICATION/DOWNGRADING SCHEDULE
16. DISTRIBUTION STATEMENT (of this Report) Approved for public release; distribution unlimited.		
17. DISTRIBUTION STATEMENT (of the abstract entered in Block 20, if different from Report) NA		
18. SUPPLEMENTARY NOTES The view, opinions, and/or findings contained in this report are those of the author(s) and should not be construed as an official Department of the Army position, policy, or decision, unless so designated by other documentation.		
19. KEY WORDS (Continue on reverse side if necessary and identify by block number) carbon fibers, torsional modulus, damping, diamagnetism, SEM, electrical resistance, resistance temperature dependence, piezoresistance		
20. ABSTRACT (Continue on reverse side if necessary and identify by block number) Microstructures and structural development with heat treatment of carbon fibers from pitch, rayon, polyacrylonitrile and pitch mesophase were characterized by diamagnetic susceptibility and SEM; and the dynamic torsional behavior (modulus, damping at about 1 Hz) and electrical resistance properties (resistivity, temperature dependence, piezoresistance) of individual fibers were measured and compared. A survey of the structure-dependence of the fiber properties revealed similarities that appear to be common to all stratic (hexagonal layer) carbon materials, as well as characteristic differences associated with fiber precursor type and processing.		

INTRODUCTION

Carbon fibers have been the subject of extensive development and research effort for about the last 15 years. The primary source of this interest is, of course, the excellent specific mechanical properties that can be achieved, and their application in high performance composite materials. Consequently, fiber properties and their dependence on microstructure, as influenced by precursor (raw material) type and processing, have considerable engineering relevance. In addition to this strong practical importance, fibers are very interesting research materials for investigating fundamental structure/property characteristics of carbons and graphites, for they are immediate members of the same stratic (hexagonal layer) carbon family that includes the common "bulk" forms (electrographites, pyrocarbons, glassy carbons, etc.).

On one hand, fibers exhibit some special characteristics, associated with their fibrous form and their processing to produce high axial property levels, that are not generally found in bulk materials: In particular, microstructures combining a very high degree of uniaxial layer orientation with small apparent layer size and little or no three-dimensional crystallinity (layer stacking order) are common; and a variety of transverse orientation textures (random, radial, circumferential) can be obtained. The fiber form is also convenient for many physical measurements, even though the required micro-manipulation techniques are tedious. On the other hand, fibers are available (either commercially or as laboratory preparations) representing all three of the major categories of carbon materials classified according to precursor type and pyrolysis behavior: Graphitizable mesophase carbons (fibers from pitch mesophase; needle cokes, pitch binder carbon, etc.); difficult-to-graphitize polymeric carbons (fibers from pitch, rayon, polyacrylonitrile; glassy carbons, chars, etc.); and CVD/vapor-grown carbons (graphite whiskers and vapor-grown fibers; pyrocarbons). Thus, the study of fibers can contribute to fundamental understanding of a broad range of bulk carbon materials as well as an increased scientific basis for fiber production and application.

The research accomplished under this grant has focussed on the investigation of several carefully selected structure-sensitive properties and their relationship to fiber microstructure. The properties studied -- torsional mechanical behavior, electrical resistance characteristics and diamagnetic susceptibility -- were chosen on the basis of the relatively small amount of information available on them and the promise that they could provide valuable insights into the nature of carbon fibers. The torsional (longitudinal shear) and electrical properties also have direct applications relevance. Fibers from pitch mesophase (PM) were of particular interest because little was known about the behavior of this most recently developed member of the carbon fiber family and their microstructures differ significantly from those of the more common fiber types. Representatives of the more familiar fibers made from isotropic pitch (P), rayon (R) and polyacrylonitrile (PAN) were also studied to provide a variety of microstructural types and to make the investigation more complete with regard to commercially important materials. Vapor-grown fibers were not studied. Isochronal (30 min) heat treatments at temperatures (HTT) ranging from ≈ 1000 to ~ 3000 C were used to induce structural evolution.

The philosophy adopted was to survey a wide range of fiber structures with the same apparatus and techniques, thereby facilitating comparisons and minimizing the influence of possible systematic errors. Reasonable precautions were taken to ensure measurement accuracy, but no attempt was made to accumulate statistically meaningful bodies of data on particular fiber types or processing variations. The objective was to determine the general patterns of behavior and their relation to structure; and there was no emphasis on cataloging behavior anomalies.

This grant supported the Ph.D. dissertations of S. Srinivasagopalan [1] and K. Komaki [2], and resulted in three senior-project theses [3-5], five papers published in conference proceedings [6-10] and two journal publications [11,12]. Eight oral presentations were made at technical conferences, and several additional publications are anticipated. The major results are reviewed and summarized below with particular attention to material not yet published.

STRUCTURAL CHARACTERIZATION

Debye-Scherrer X-ray diffraction films and optical microscopy generally confirmed information available from the literature. More revealing insights were provided by scanning electron microscopy (SEM) and diamagnetic susceptibility measurements.

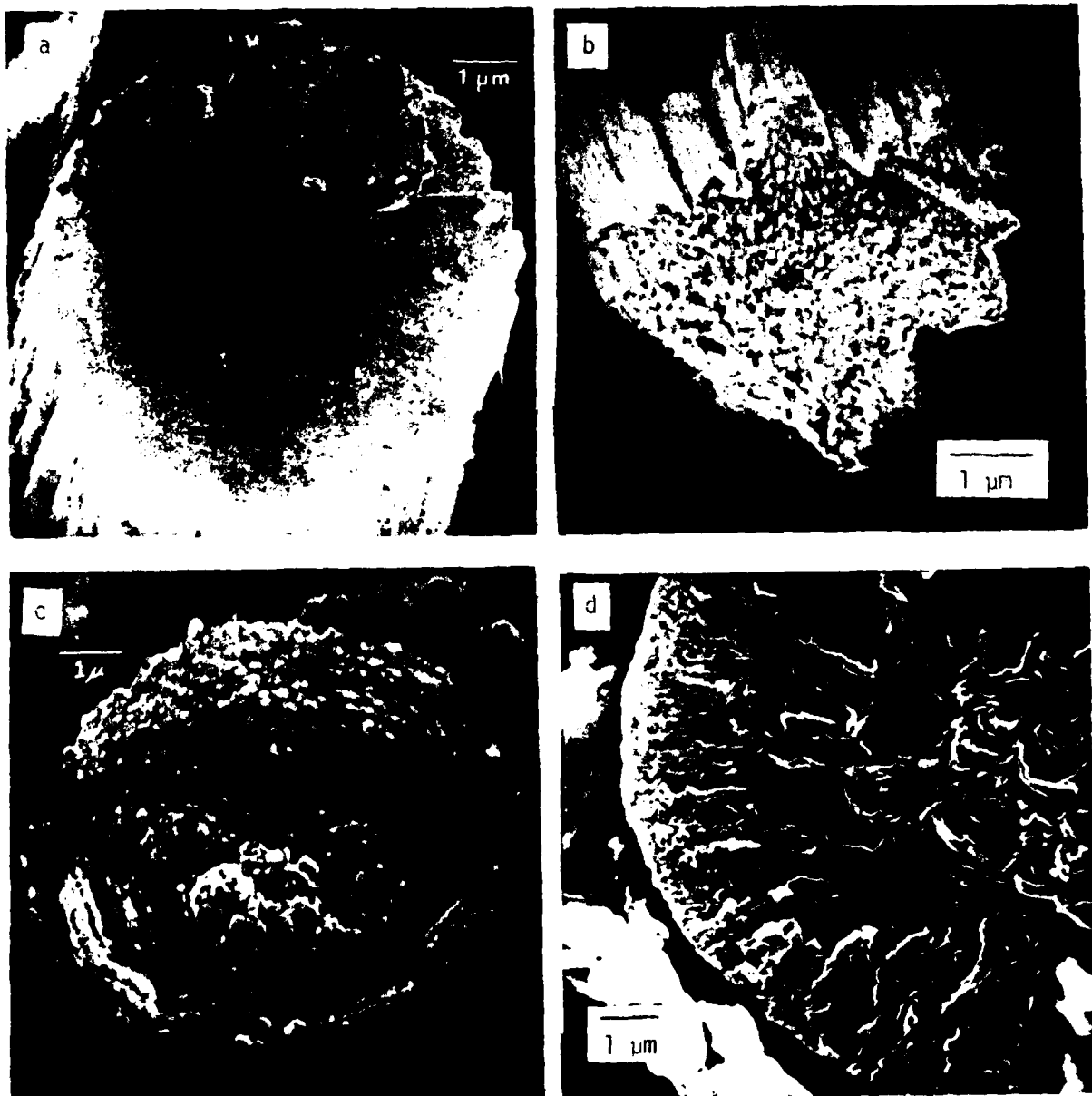


Fig. 1. Scanning electron micrographs of fiber transverse fracture surfaces: a) Carbonized PAN (T-400, uncoated); b) highly hot-stretched rayon (T-100); c) high modulus PAN with circumferential structure (Courtauld's HM-S, ~ 1969); d) ortho mesophase with radial component (Union Carbide, $E \approx 200$ GPa).

Information about fiber microstructures as well as cross section shape and size may be obtained from SEM of transverse fracture surfaces [1,7,10-12]. Image definition is often poor and charging effects are sometimes bothersome for bare (uncoated) fibers. Thin evaporated or sputtered Pd or Au coatings greatly improve image quality by increasing secondary electron emission and reducing charging. However, coating often produces fine nodular (a few hundred nm diameter) artifact textures on the fracture surfaces, and these must not be confused with the true substructure of the carbon. In general, the fracture surfaces of carbonized fibers from all precursors are quite smooth in appearance and the only prominent features are fractographic in origin. This is illustrated by the uncoated medium-modulus (230 GPa) PAN fiber shown in Fig. 1a. However, in fibers from rayon and PAN there is often a suggestion of a very fine granular texture that becomes more clearly defined after processing to high heat treatment temperatures (HTT) or hot-stretching and has often been cited as evidence of a fibrillar substructure. The highly hot-stretched rayon fiber ($E = 680$ GPa) shown in Fig. 1b exhibits such fibrillar features (~ 80 nm diameter) in the core, as well as a surface sheath about 120 nm thick with unresolved structure. The somewhat coarser granularity on the type I PAN fiber fracture in Fig. 1c is probably a coating artifact, but it "decorates" an unusually extensive circumferential layer texture. In contrast, the fracture textures of PM fibers ($HTT \geq 1500$ C) are obviously and rather coarsely laminar and graphitic, commonly consisting of crinkled layer packets ≤ 100 nm thick and ≥ 500 nm wide. This is illustrated in Fig. 1d ($HTT \sim 1800$ C) which shows a "random" scroll texture in the center and a radial orientation in the outer portions. In strongly radial PM fibers with missing-wedge cracks extending to the center of the cross section, the average wedge angle increases with HTT (e.g., from ≤ 90 deg for $HTT \sim 1000$ to ≈ 180 deg for ≥ 2500 C) [4]. At $HTT \geq 2200$ C, PM fibers graphitize, and the fracture surfaces become rougher due to increased longitudinal (interlaminar) splitting. No evidence of surface sheaths was detected in SEM observations on PAN or PM fibers.

The diamagnetic mass susceptibility, measured in the axial (X_A) and radial (X_R) directions on small bundles of parallel fibers, provides qualitative information about layer-structure development and semi-quantitative data on axial layer preferred orientation [3,10,11,13]. A "crystallinity"/texture diagram [10,14,15] is generated by plotting X_R against X_A as shown in Fig. 2a. Layer size and perfection, measured by the tensor trace ($X_T = X_A + 2X_R = X_C + 2X_a$ where X_a , X_C are the "crystallite" susceptibilities parallel and perpendicular respectively to the layers) increases radially outward from the origin in the absence of stacking order; the development of layer stacking order causes displacement toward the origin when layer size is sufficiently large (graphitization is often signalled by a X_T maximum). The dashed "crystalline hexagonal graphite" boundary at $X_T = 22$ is one of an infinite family of parallel iso- X_T lines. Axial orientation texture ($R_z = \sin^2 \phi$ where ϕ is the angle between the fiber axis z and the crystallite c axes) increases counterclockwise. Quantitative orientation values depend on the assumptions that the structure is homogeneous and the structure sensitivity of the diamagnetism resides entirely in X_C . The arrows on the data curves indicate increasing HTT (typically over the range 1000 to 3000 C).

The magnetically-inferred structural development in fibers from P and R is very similar to that of glassy carbons. They are non-graphitizing, and P fibers remain isotropic, but a little anisotropy develops in R fibers. Hot-stretching (H-S) greatly increases the orientation texture (and hence E) of these fibers and also improves the effective layer size/perfection without generating stacking order. The fibers from PM are very anisotropic, and both structural perfection and orientation increase rapidly with HTT (> 1600 C for the data shown). X_T passes thru a maximum near $HTT \approx 2300$ C, indicating the onset of stacking order (confirmed by XRD). Residual nitrogen defects, which anneal at $HTT \leq 1800$ C,

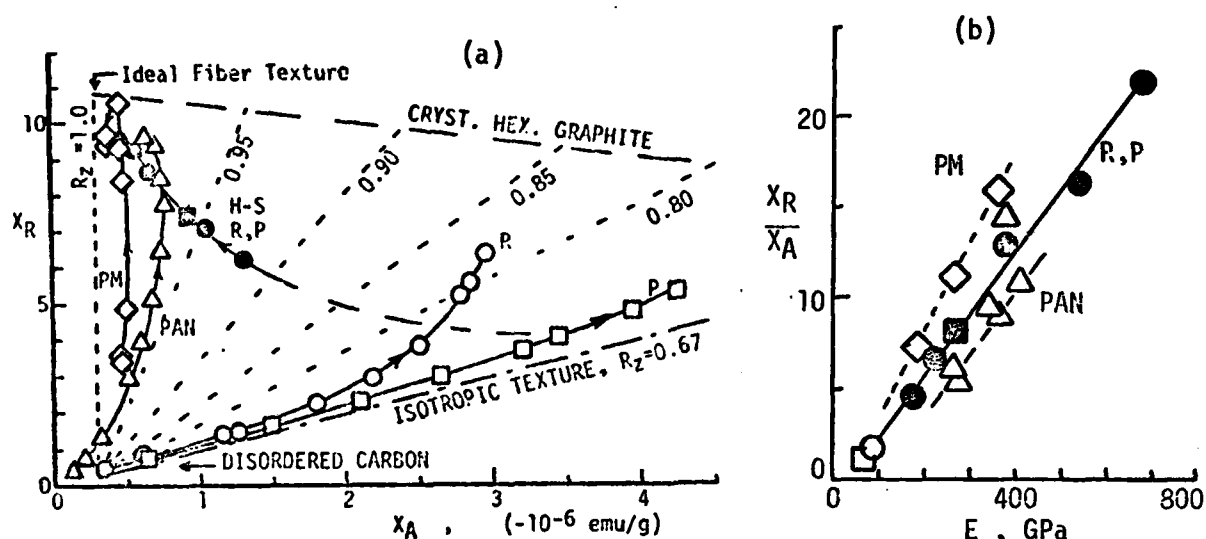


Fig.2. a) Diamagnetic susceptibility crystallinity/texture diagram for fibers from pitch mesophase, PAN, rayon and pitch. Arrows show direction of increasing heat treatment; solid points indicate hot-stretched. b) Magnetic anisotropy ratio as a function of nominal Young's modulus for as-processed fibers.

quench the diamagnetism in carbonized fibers from PAN and the low HTT data points fall outside the valid region of the diagram. Defect annealing and layer structure development is very similar for PAN fibers from different sources; X_T approaches a maximum at the highest HTT, indicating incipient graphitization (little or no evidence of stacking order is found by XRD). The anisotropy, which is lower than that of PM fibers, increases with $HTT \geq 2400$ C but the magnitudes depend on fiber source, evidently as a result of differences in precursor, stabilization or carbonization processing. The data in Fig. 2a are for a low-anisotropy PAN (Hercules A-S); the path of high anisotropy fiber (Union Carbide T-400) lies close to the PM path, crossing it at both low and high HTT.

When the anisotropy ratio X_R/X_A (another measure of preferred orientation) is plotted against axial Young's modulus, as shown in Fig. 2b for as-received fibers, it is evident that the degree of orientation required for a given modulus value generally increases in the order PAN, hot-stretched R and P, PM. This may be attributed to an effective interlayer shear compliance that increases in the same order and acts to "short circuit" the very low in-plane compliance. On the basis of graphitizability, one might expect the ranking of PAN and R,P to be reversed. Apparently, the hot-stretching required to achieve high orientation in the latter acts to reduce inherent morphological constraints (such as layer-ribbon intertwining) that inhibit shear in difficult-to-graphitize carbons. This interpretation is consistent with the torsional results described below that show that the longitudinal shear modulus increases in the PM, R, P, PAN. It may prove more difficult to achieve consistent high strength levels in the graphitizable PM fibers because of their higher intrinsic shear compliance; large stress concentrations can build up at the boundaries of misoriented regions.

DYNAMIC TORSIONAL MODULUS AND DAMPING

Prior to the initiation of this grant, vacuum double-ended torsion pendulum techniques for room temperature measurements at ~ 1 Hz and very low dynamic surface shear strains ($\sim 10^{-5}$) on single carbon fibers under adjustable static tensile stress and/or torsional bias strain were developed here and used to survey the torsional behavior of as-received commercial fibers from P, R and PAN [16-18].

A residual pressure of $\approx 10^{-3}$ Pa is required to reduce the gas damping background to an acceptable level. Fused silica fiber was used as an isotropic elastic reference material. During the tenure of the present grant, the equipment was modified to improve frequency measurement precision, new apparatus was built to investigate the dependence of the torsional modulus G and the damping (logarithmic decrement, δ) on measurement temperature, the study was extended to pitch mesophase fibers and to the influence of HTT on the characteristics of all carbon fiber types, and the application of anisotropic elastic theory to interpretation of the results was explored [1,7]. Perhaps the most surprising of several unanticipated results was the discovery that the torsional behavior of PM fibers is quite similar to that of other carbon fiber types, despite the very significant differences in microstructure and graphitizability. The apparent G value (proportional to the square of the frequency) increases with static tensile stress (a solid mechanics effect resulting from the additional unwinding torques) but damping is generally unaffected. Static torsional bias strain produces very interesting effects, discussed later, that are attributed to decoupling between fiber substructure elements.

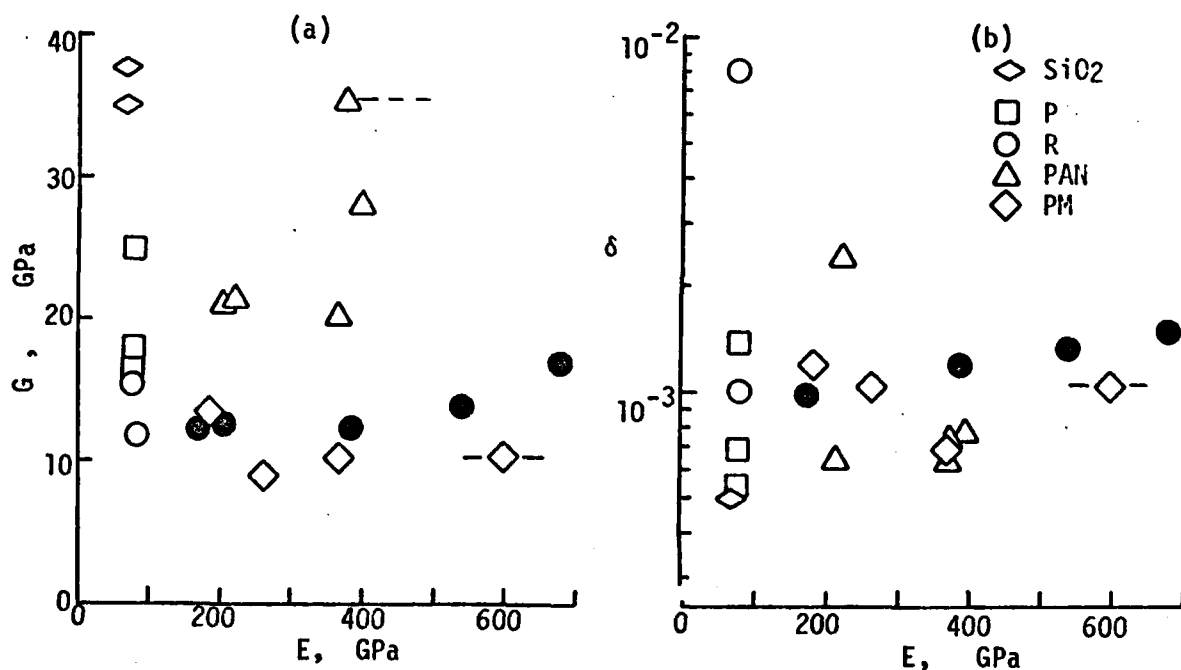


Fig. 3. a) Torsional modulus G (linear scale) and b) log decrement δ (log scale) plotted against fiber tensile modulus E .

Representative data for G and δ , extrapolated to zero static strain, are plotted against Young's modulus as a display parameter in Fig. 3a,b. The maximum processing temperatures for these fibers range from ~ 1000 to > 2700 C. Fiber G values are low (9 to 35 GPa, much smaller than E) and generally insensitive to E ; but there is a correlation with fiber type (G increases in the order PM, R, P, PAN), and a fairly wide range of values (18-35 GPa) occurs in fibers from PAN. Damping is typically low ($\delta \approx 10^{-3}$) except for carbonized R and some medium- E carbonized PAN where it can be an order of magnitude higher, and it is independent of strain amplitude at the low dynamic measurement levels used.

Several factors in addition to precursor type contribute to the observed data spread: G values were computed from measured parameters (frequency, fiber length and cross section area, bob moment of inertia) and there is an estimated uncertainty in absolute value of $\approx 15\%$ for circular section fibers (P, PM, PAN)

due mainly to uncertainties in area determination. For the irregularly shaped rayon fibers (cf Fig. 1b), G was computed from the equivalent circular area and there is an additional systematic underestimation of uncertain magnitude. From this it is concluded that the true shear modulus of R is definitely higher than that of PM. The torsional behavior is dominated, of course, by the properties of the material near the fiber surface. The increase in G and δ in highly hot-stretched R may be associated with the formation of a surface sheath (Fig. 1b). Because of the elastic anisotropy of graphite, layer orientation texture plays a very strong role in determining the fiber moduli: As is well known, the tensile modulus depends primarily on the degree of axial orientation. Similarly, the torsional modulus depends on the transverse orientation texture [1,7,12]. The lowest G value was obtained for the PM fiber with appreciable radial orientation (Fig. 1d) where the large interlayer shear compliance dominates the behavior. The highest G value occurred in the PAN fiber with the pronounced circumferential texture (Fig. 1c); here the very much lower intralayer shear compliance would be determining if the layer shells were continuous. The fibers with intermediate G values have more random transverse textures.

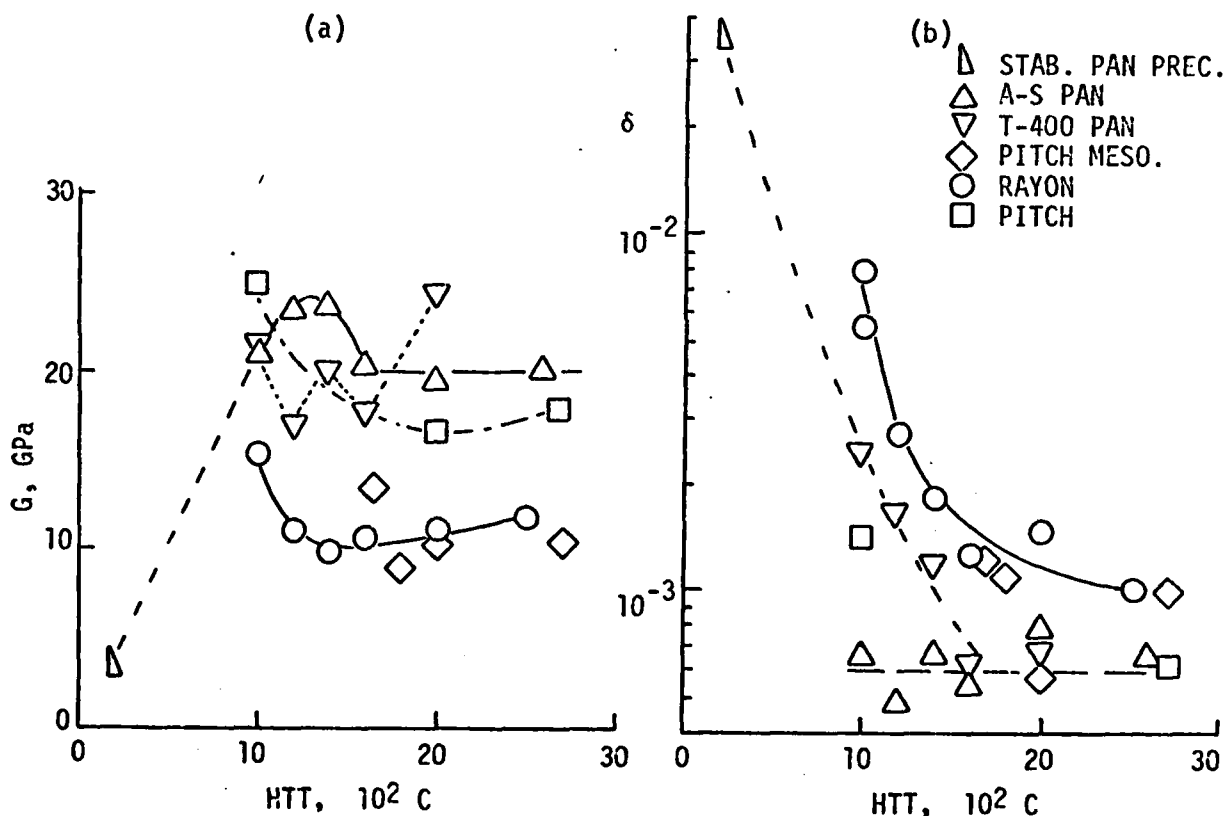


Fig. 4. Influence of heat treatment temperature on a) torsional modulus (linear scale) and b) damping (log scale).

Some results on the effect of isochronal (30 min) HTT on G and δ are shown in Fig. 4a,b. For all fiber types, high damping values anneal in the range <2000 C while the δ of low-loss fibers is unaffected. This indicates a dependence of δ on point or other localized defects that anneal readily. The effect of HTT on G is more varied and complex: The small maximum near 1300 C for Hercules A-S confirms results obtained elsewhere [19] on similar (British precursor) fibers. However, this behavior is evidently not a universal characteristic of PAN since T-400 (Japanese precursor) does not show it. For low-E rayon (Union Carbide T-11), G decreases in the ≤ 1500 C range as δ decreases, but tends to increase again at high HTT; and there is evidence of similar behavior in pitch (Kreha)

and pitch mesophase. Published information on temperature-dependent damping effects in carbon materials is both sparse and confused, but there is evidence that damping maxima can occur in bulk carbons and perhaps in fibers. However, no appreciable variation in fiber G or δ were found here over the measurement range from about -50 to $+50$ C. Investigation over a broader range was prevented at higher temperatures by the intrusion of large glass transition effects (δ increase and G decrease) in the epoxy cement used to attach the fibers, and at both ends of the range by large temperature gradients resulting from poor heat transfer in the vacuum apparatus.

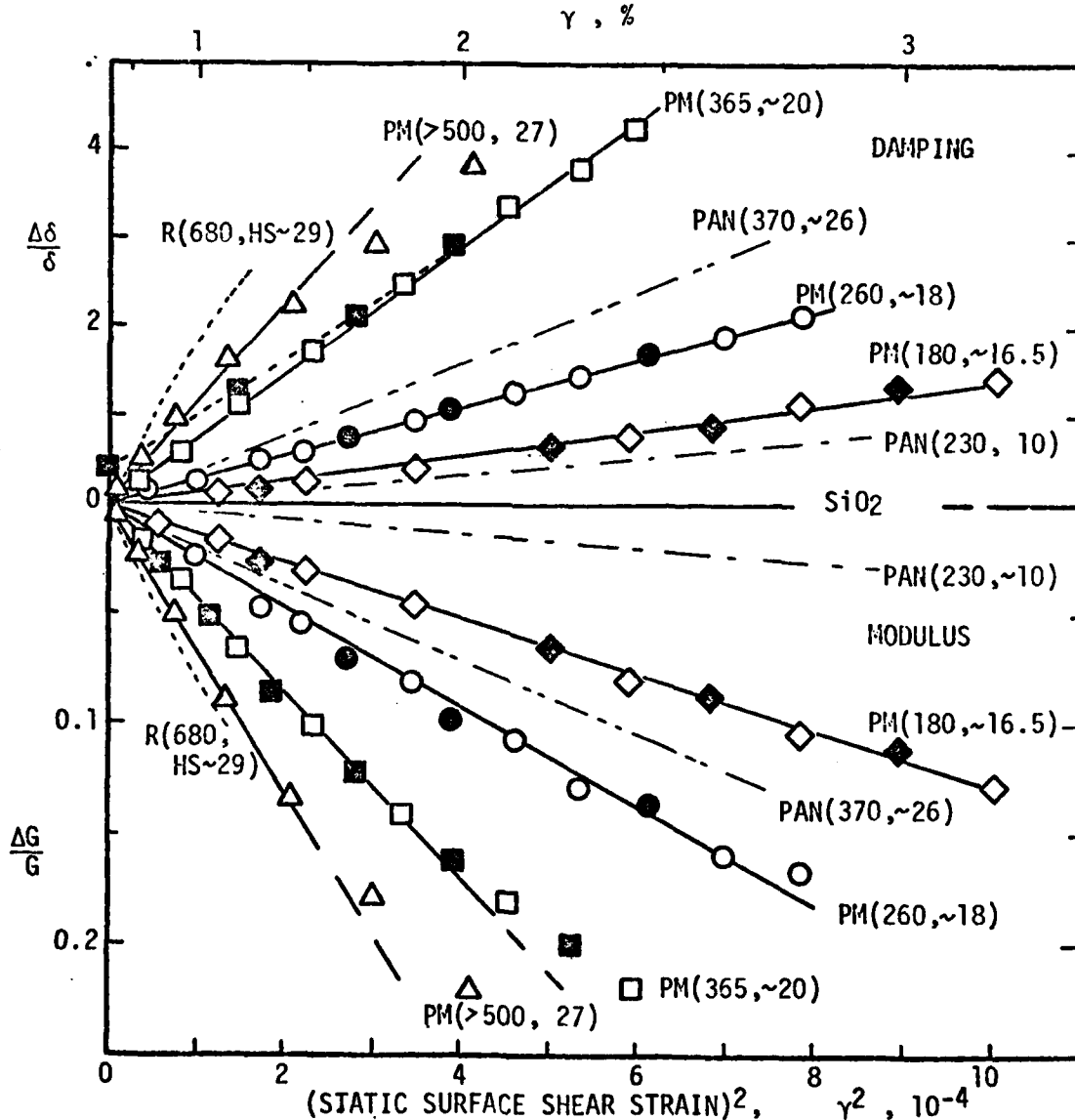


Fig. 5. Fractional increase in damping and decrease in torsional modulus with the square of the static bias shear strain γ (open symbols, increasing; solid, decreasing γ). E in GPa and HTT in 100 C in parentheses.

When carbon fibers are subjected to large static torsional bias strains γ the torsional modulus decreases and damping increases approximately linearly with γ^2 as shown in Fig. 5. These effects are substantially reversible (no residual change in G ; residual δ increases are small and decay with time after unloading) and increase in magnitude with increasing HTT (or hot stretching) in all types

of carbon fibers; but they do not occur in silica fibers (isotropic elastic theory predicts a very small G increase which was not observed). These phenomena are attributed to elastic decoupling between fibrillar (or other) substructural units in the carbon fibers. By analogy with the characteristics of multi-strand torsional suspensions, it was inferred that coupling is relatively tight and the amount of decoupling required to produce the observed effects is small. Furthermore, the apparent insensitivity of these phenomena to significant microstructural differences may be rationalized since similar characteristics may be obtained with a large number of small, high G stands (R,PAN) or a smaller number of larger strands with lower G values (PM) [7].

ELECTRICAL RESISTANCE BEHAVIOR

One of the initial objectives of this grant was to study the influence of mechanical stress on the electrical resistance (i.e., the piezoresistance) of carbon fibers. In the course of these studies considerable information was obtained on the resistivity and on the temperature dependence of resistance as well.

Interest in carbon fiber resistance characteristics has greatly increased since the initiation of this project because of the recognition that serious hazards can result from the infiltration of dispersed fibers into electrical apparatus [20]. Our results show that fiber resistances range from ≥ 12 to ≤ 0.2 k-ohm/cm depending of diameter, precursor type and processing/HTT. However, the development of the resistivity ρ with HTT is very similar to that in bulk carbons with comparable structures and there are few surprises in this aspect. The ρ values of fibers processed between ~ 1000 and 3000 C range over about two orders of magnitude (0.1 to 10 milli ohm-cm), bounded by isotropic, hard-to-graphitize pitch fibers (like glassy carbon) at the top and by anisotropic, graphitizable pitch mesophase fibers (somewhat higher than pyrographite) at the bottom. The parallel-to-layer resistivity of single crystal graphite is 0.04 milli ohm-cm. Following a large and precipitous drop in the < 1200 C HTT range, representing the insulator/conductor transition associated with carbonization, ρ levels out (P fiber, glassy carbon), or decreases further as defects anneal and orientation texture increases (R, PAN, PM fibers and pyrocarbons) and stacking order develops (PM fiber, electrographite, pyrocarbon). Layer structure development and orientation texture have roughly equal influence in determining ρ . Interestingly, the annealing of nitrogen defects in PAN has no obvious influence on the resistivity though there is a large effect on magnetic behavior. Despite the wide ρ range that is obtainable, one milli ohm-cm (10 times that of Nichrome resistance wire) is a good round-number figure for practical use: Fibers from PAN, PM and R (hot stretched) with $E \approx 400$ GPa (58 Mpsi) all have ρ within 20% of this value. For carbonized PAN fibers in the $E \approx 200$ GPa range, ρ is 2-3 milli-ohm-cm, but it could be driven much higher if processing temperatures could be dropped well below 1000 C without sacrificing mechanical properties.

The temperature dependence of the resistance is always negative for fibers, but its development with HTT is very interesting [2,8,10,21,22]. We have measured it both by the temperature coefficient of resistance, $TCR = d \ln R / dT$ over the 0 to $+50$ C range, and by the ratio of the resistance at liquid nitrogen temperature to that at 0 C as shown in Fig. 6. The negative temperature dependence decreases to a minimum then increases toward a maximum as HTT and structural perfection increase. Resistance ratio data for a wide variety of bulk carbon materials can be extracted from the literature and there are close analogies to fiber behavior: PM fiber is similar to "soft" coke filler/pitch binder carbon [23], PAN fiber is like a "hard" glassy carbon filler/resin binder carbon [23], and R and P fibers are very similar to glassy carbons [24]. The temperature dependence of hot-stretched R,P is similar to that of PAN. Ultimately, the temperature dependence must drop and reverse sign (at least for highly oriented materials) because the parallel-to-layer dependence in crystalline graphite is positive. This does not

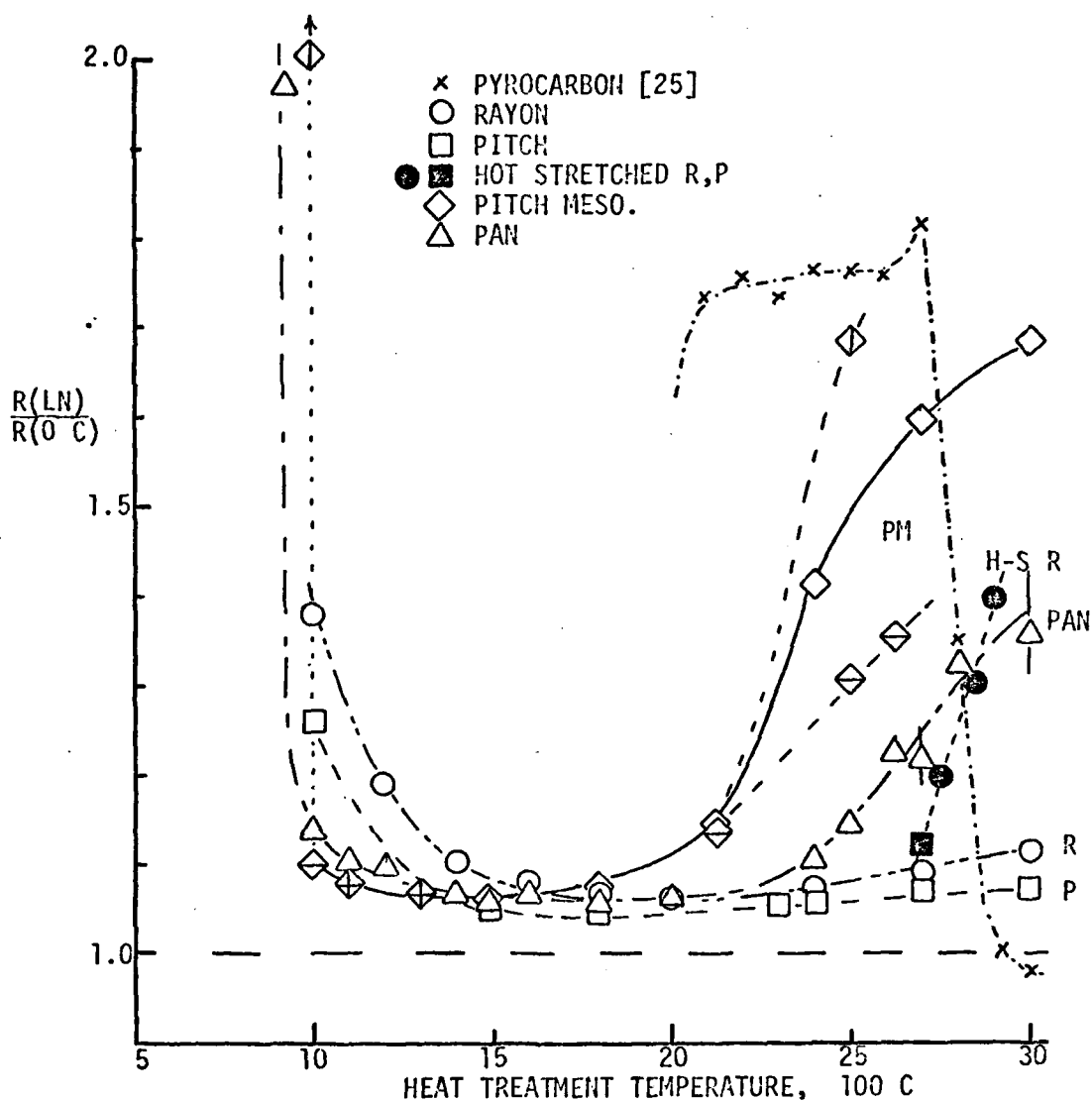


Fig. 6. Resistance ratio as a function of heat treatment temperature.

happen for any of the fibers studied here, but does occur in pyrocarbon [25]. The behavior of $-TCR$ is similar but not identical to that of the resistance ratio because the shape of the R vs T curve depends on carbon type and processing. For carbon fibers, a plot of $-TCR$ against resistance ratio deviates greatly from linearity in the direction corresponding to positive curvature d^2R/dT^2 at both the high and the low-ends of the structural perfection (HTT/graphitization) scale, and there is a small negative-curvature deviation over much of the intermediate range.

The temperature-dependence curves (Fig. 6) have similar shapes and minima for fibers from different precursors, but the response to HTT is "stretched out" with decreasing graphitizability. It appears that a single universal curve might result if the data were plotted against the proper structural characterization parameter. The fiber data allow convenient comparison of the temperature dependence over a wide range of structures, but the observed behavior is not

unique to fibers. It appears to be common to all stratic carbon materials, and associated primarily with layer structure development rather than stacking order or orientation texture, although this does not appear to have been widely appreciated. These effects are not yet understood, but McClure [26] has proposed a reasonable phenomenological description based on positive carrier density and negative mobility temperature dependences that develop in different ways with increasing HTT. His interpretation and our observations suggest the following general relationships with structure: The initial decrease of negative dependence to a minimum may be associated with the annealing of point defects (including residual H,N, etc.) that can act as shallow carrier traps. The subsequent increase toward a maximum accompanies increasing layer size/perfection (characteristic of incipient graphitization) that primarily affects scattering processes. The final drop and sign reversal is associated with a combination of large layer size/perfection and a high degree of preferred orientation; graphitization may be necessary but it is not sufficient. This suggests that a change in scattering processes is responsible here too. The resistance temperature dependence is a useful empirical structural characterization parameter [21,22] and may prove to be a powerful investigative tool when better understood.

Very little is known about the tensile piezoresistance behavior of bulk carbon materials, but this property can be measured easily on fibers [2,6,9,10, 27,28] and some interesting characteristics are observed. As shown by the representative results in Fig. 7a the qualitative pattern of behavior is remarkably similar for all precursor types despite the differences in microstructures: For most fibers (low to medium-high E) the effect is positive and generally approximately linear with strain ϵ . The slope $S = d \ln R / d \epsilon$ lies in the range from ~ 2.5 to ~ 1 , decreasing with increasing HTT and structural development. However, for sufficiently high orientation texture and/or structural perfection ($E \geq 500$ GPa for hot-stretched R; $HTT \geq 2200$ C for PM and ≥ 2700 C for PAN), S becomes negative at low ϵ , but tends to turn positive again at high ϵ . This transition from plus to minus behavior is rather abrupt as a function of HTT (or hot-stretching) for particular precursor types, and as a function of ρ for all fiber types as shown in Fig. 7b. The piezoresistance is reversible in both the plus and minus regimes if the failure strain is not approached too closely. At liquid nitrogen temperature the response is modified as though a small tensile bias strain were present (especially for well-oriented fibers). This is qualitatively consistent with the expected effects of the small negative parallel-to-layer and large positive perpendicular-to-layer thermal expansion coefficients.

These results suggest that the piezoresistance may be modeled as an additive combination of a positive component and a negative component that saturates at high ϵ . With the assumptions that the influence on effective fiber resistivity of internal contacts between substructure units can be represented by a strain-dependent coefficient $C(\epsilon)$, and that the c-axis conductivity of the "crystallites" is negligible compared with the conductivity parallel to the layers, it can be shown by logarithmic differentiation of the definition of wire resistance that a number of different positive and negative effects may contribute:

$\delta R/R = +(1 + 2\nu)\epsilon$	geometrical term depending on Poisson's ratio ν ; magnitude $\leq 2\epsilon$ for ideal isotropic materials ($\nu \leq 0.5$)
$\pm \delta C(\epsilon)/C(\epsilon)$	effect of internal contact opening (+) or closing (-)
$-\delta R_z/R_z$	strain-induced layer orientation increase; $R_z = \sin^2 \phi$ where ϕ is the angle between the fiber axis \bar{z} and the crystallite c axes
$\mp \delta \mu/\mu$	carrier mobility increase (-) or decrease (+) (scattering decrease or increase)
$\pm \delta n/n$	carrier density decrease (+) or increase (-)

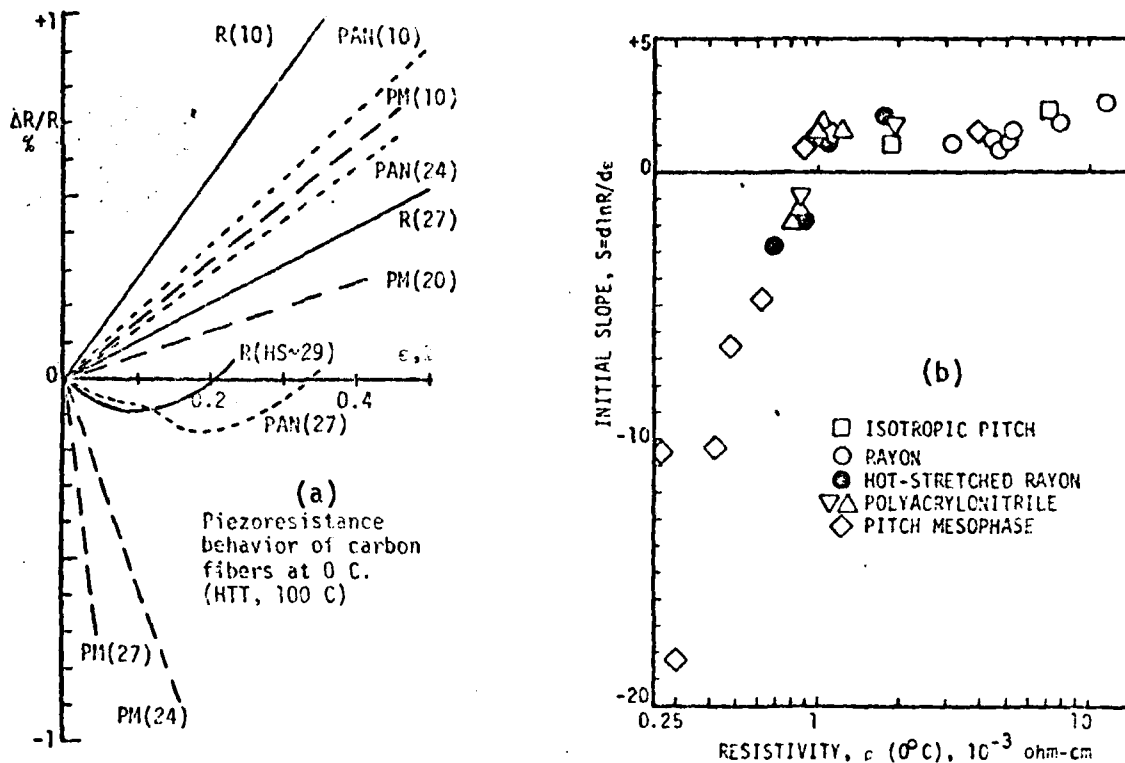


Fig. 7. a) Fractional resistance change with tensile strain. Heat treatment temperature in 100 C in parentheses. b) Initial slope as a function of fiber resistivity.

Evaluation of the relative importance of these various contributions is more difficult. The geometrical effect probably dominates the positive behavior of carbonized and low modulus fibers, but it must be augmented by other positive contributions such as contact opening, carrier density decrease or scattering increase. The importance of internal contact effects may be questioned because of the relative insensitivity of the piezoresistance behavior to microstructural type; however, they are probably responsible for the positive up-turn which commonly precedes failure. Stress-induced orientation occurs in fibers [29] and could contribute a saturable structure-dependent negative component. However, both positive geometrical and negative layer orientation effects would be expected to diminish in importance as the intrinsic structural anisotropy increases: When a-direction conduction is strongly preferred, the effective conduction path should be insensitive to layer unwrinkling and the accompanying transverse contraction and axial elongation of the fiber (considerable axial continuity of the layers can be inferred from the microstructures and high mechanical properties). However, layer straightening should decrease scattering (increase effective mobility) and this may be the primary origin of the large negative piezoresistance in graphitized PM. The piezoresistance is less sensitive to fiber type than anticipated at the initiation of this investigation; but it is remarkably sensitive to structural development in the incipient-graphitization range where the sign reverses. Further studies will be required to permit confident interpretation of the piezoresistance behavior.

REFERENCES

1. Seshadri Srinivasagopalan, "Dynamic torsional behavior of some carbon fibers", Ph.D. Dissertation, University of Washington, Sept. 1979
 2. Kunio Komaki, "Effects of stress and temperature on the electrical resistance of carbon fibers", Ph.D. Dissertation, Univ. of Washington, May 1980
 3. Douglas W. Gilbert, "Graphitization of carbon fibers", Senior Project Thesis, Ceramic Engineering, Univ. of Washington, June 1977
 4. Roy J.G. Baumer, "Optical microscopy techniques for use in the study of carbon materials", Senior Project Thesis, Ceramic Engineering, Univ. of Washington, June 1980
 5. Richard A. Brown, "Electroplating of copper on carbon materials", Senior Project Thesis, Ceramic Engineering, Univ. of Washington, Summer 1980
 6. D. B. Fischbach & Kunio Komaki, "Piezoresistance of carbon fibers", Ext. Abs. & Program, 13th Biennial Conf. on Carbon, Amer. Carbon Soc. (Univ. of Calif., Irvine, July 1977) pp130-1
 7. D.B. Fischbach & S. Srinivasagopalan, "Dynamic torsional behavior of carbon fibers from pitch mesophase", Proc. 5th London International Carbon and Graphite Conf. (Imperial College, Sept. 1978), Society of Chemical Ind., London, 1978, Vol.I, pp 389-97
 8. D.B. Fischbach & Kunio Komaki, "Electrical resistance of carbon fibers", Ext. Abs. & Program, 14th Biennial Conf. on Carbon (Penn.State Univ., June 1979), Amer. Carbon Soc., pp 191-2
 9. Kunio Komaki & D.B. Fischbach, "Experimental observations on carbon fiber piezoresistance behavior", ibid. pp 193-4
 10. D.B. Fischbach, "Observations on the properties and structure of carbon fibers", Carbon '80 Preprints, 3rd International Carbon Conf. (Baden-Baden, F.R.G., July, 1980), Arbeitskreis Kohlenstoff der Deutschen Keramischen Gesellschaft, pp. 590-3
 11. D.B. Fischbach & D.W. Gilbert, "Diamagnetic characterization of carbon fibers from pitch mesophase, pitch and polyacrylonitrile", J.Mater.Sci. 14 (7) 1586-92, July (1979); also, cover photo for this issue.
 12. D.B. Fischbach, S. Srinivassgopalan, A. Schmidt, L. Kniffen, "Carbon fiber rigidity", Ceramic Abs. 58 (7/8) July/Aug.(1979), back cover photo (Ceramo-graphic Exhibit poster)
- Note: All of the above resulted from this grant.
13. C.B. Scott & D.B. Fischbach, "Diamagnetic studies on as-processed carbon fibers", J. Appl. Phys. 47 (12) 5329-35 (1976)
 14. D.B. Fischbach, "Characterization of carbon materials by diamagnetic susceptibility", Proc. 5th London International Carbon and Graphite Conf, Society for Chemical Industry, London, 1978, Vol.II, pp 885-90
 15. D.B. Fischbach, "Diamagnetic crystallinity/texture diagram for carbon materials", Ext. Abs. & Program, 14th Biennial Conf. on Carbon, June 1979, pp 101-2
 16. Roy E. Henrichsen, "Dynamic torsional response of individual carbon fibers", Ph.D. Dissertation, Univ. of Washington, 1976; (Dissert.Abs.Int. 37B (5) 2396, Nov. 1976; order #76-25,416)
 17. R.E. Henrichsen & D.B. Fischbach, "Torsional modulus and damping of carbon fibers", Proc. 4th London International Carbon and Graphite Conf. (1974), Society of Chemical Industry, London, 1976, pp 626-33

18. R.E. Henrichsen & D.B. Fischbach, "Torsional non-linear elasticity and damping of carbon fibers", Ext. Abs. & Program, 12th Biennial Conf. on Carbon (Univ. of Pittsburgh, 1975), pp 105-6
19. R.D. Adams, "The dynamic longitudinal shear modulus and damping of carbon fibres", J.Phys.D: Appl.Phys. 8 738-48 (1975)
20. Office of Naval Research Fiber Study Group, "Carbon fiber electrical resistance modification -- its relationship to electrical equipment malfunction", ONR Final Rept. 039-160-2, 1 Sept. 1978
21. D. Robson, F.Y.I. Assabghy & D.J.E. Ingram, "Some electronic properties of polyacrylonitrile-based carbon fibres", J.Phys.D:Appl.Phys. 5 169-79 (1972); with E.G. Cooper, "Electronic properties of high-temperature carbon fibres and their correlations", ibid. 6 1822-34 (1973)
22. A.A. Bright & L.S. Singer, "The electronic and structural characteristics of carbon fibers from mesophase pitch", Carbon 17 59-69 (1979)
23. M. Inagaki, Y. Komatsu & J.V. Zanchetta, "Hall coefficient and magneto-resistance of carbons and polycrystalline graphite in the temperature range 1.5 - 300 K", Carbon 7 (1) 163-75 (1969)
24. T. Yamaguchi, "Galvanomagnetic properties of glassy carbon", Carbon 1 (1) 47-50 (1963)
25. S. Gromb, "Etude de proprietes electroniques de pyrocarbones", J. Chimie Physique, 864-77 (1964)
D.B. Fischbach, unpublished data
26. J.W. McClure, Univ. of Oregon, private communication, 1979
27. C.N. Owston, "Electrical properties of single carbon fibres", J.Phys.D: Appl.Phys. 3 (11) 1615-26 (1970); P.C. Conor & C.N. Owston, "Electrical resistance of single carbon fibres", Nature 223 1146-7 (1969)
28. C.A. Berg, H. Cumpston & A. Rinsky, "Piezoresistance of graphite fibers", Textile Res. J. 42 486-9 (1972)
M. Endo & T. Koyama, "Piezoresistance effect of carbon fibers prepared by thermal decomposition of benzene", Ext. Abs. & Program, 14th Biennial Conf. on Carbon (Penn.State Univ., June 1979) pp 258-9
29. G.J. Curtis, J.M. Milne & W.N. Reynolds, "Non-Hookean behavior of strong carbon fibres", Nature 220 1024-5 (1968)

SCIENTIFIC PERSONNEL (who received financial support from this grant)

Seshadri Srinivasagopalan, Research Assistant, Ph.D. 1979
 Kunio Komaki, Research Assistant, Ph.D. 1980
 David B. Fischbach, Principal Investigator
 Research Professor, Ceramic Engineering

Accession For	NTIS GRAB	By	Distribution/	Availability/	Avail and/or
	DDC TAB				special
Unannounced					
Justification					
					Dist
					A